DOI: 10.24874/ti.1770.10.24.12

Tribology in Industry

www.tribology.rs

RESEARCH

Enhancing Mechanical and Tribological Properties of 3D-Printed Dental Photopolymer Resin Using Hydroxyapatite Nanoparticles

Rochmadi[a,b], Kuncoro Diharjo[a], Ubaidillah[a,c,*], Joko Triyono[a], Eko Surojo[a], Abdurrahman Hanif[a], Bhre Wangsa Lenggana[d], Seung-Bok Choi[e,f]

[a]*Department of Mechanical Engineering, Faculty of Engineering, Universitas Sebelas Maret, Surakarta 57126, Indonesia,*
[b]*Health Facilities Security Center, Surakarta 57126, Indonesia,*
[c]*Mechanical Engineering Department, Faculty of Engineering, Islamic University of Madinah, Al Madinah Al Munawwarah 42351, Saudi Arabia,*
[d]*Department of Mechanical Engineering, Universitas Jenderal Soedirman, Purwokerto, 53122, Indonesia,*
[e]*Department of Mechanical Engineering, Industrial University of Ho Chi Minh City (IUH), Ho Chi Minh City 70000, Vietnam,*
[f]*Department of Mechanical Engineering, The State University of New York, Korea (SUNY Korea), Incheon 21985, South Korea.*

Keywords:

3D printing
Composites
Nanoparticle
Hydroxyapatite
Tribometry

* Corresponding author:

Ubaidillah
E-mail: ubaidillah_ft@staff.uns.ac.id

Received: 15 October 2024
Revised: 13 November 2024
Accepted: 26 December 2024

A B S T R A C T

A novel stereolithography-based three-dimensional (3D) printing technique incorporating hydroxyapatite (HA) nanoparticles into dental photopolymer resin was introduced in this study. The design aimed to address the inadequate mechanical strength of conventional dental photopolymer resins by leveraging the reinforcing properties of HA. The HA concentrations of 0, 1, 3, and 5 wt.% were mixed with the resin to produce four distinct resin-HA (RHA) composites. The composites were evaluated for tensile strength, impact strength, and hardness, wear rate (K), and coefficient of friction (μ). Morphological analysis using scanning electron microscopy (SEM) provided insights into HA distribution and the resulting microstructural changes. The design approach incorporated HA nanoparticles to enhance molecular stiffness and promote a mechanical interlocking effect within the resin matrix. These mechanisms led to significant improvements in the composite's mechanical and tribological properties. The 5 wt.% RHA composite demonstrated the highest tensile strength (66.11 MPa), impact strength (35.2 kJ/m^2), and Shore D hardness (79.32). Tribological tests revealed that this composite also exhibited the lowest wear rate and coefficient of friction, correlating with its superior mechanical performance. SEM analysis revealed finer debris and smoother wear tracks in HA-reinforced samples compared to HA-free samples, highlighting the role of HA in improving wear resistance. This study underscores the potential of integrating HA nanoparticles to enhance the performance of 3D-printed dental resins, providing a pathway for developing advanced materials tailored for dental and biomedical applications.

1. INTRODUCTION

Additive manufacturing (AM), commonly referred to as three-dimensional (3D) printing, has transformed modern production techniques by enabling the creation of complex geometries from digital designs without the need for melds or specialised tools [1]. It has proven to be particularly beneficial in terms of design flexibility, material efficiency, and rapid prototyping compared to traditional manufacturing methods. This versatility has led to its widespread application across industries such as aerospace, automotive, healthcare, and consumer goods, where the production of lightweight and high-performance components is becoming increasingly critical. Moreover, the ability of AM to produce intricate structures that would be difficult or impossible with the use of conventional methods has paved the way for innovations such as customised medical implants and lightweight aerospace structures [1,2]. Despite these advancements, limitations related to material properties, particularly in resin-based applications, remain a significant barrier to further optimization of this technology.

Rapid prototyping, often synonymous with 3D printing, is increasingly favoured due to its reduced development time, ease of use, and low risk. Within this context, vat photopolymerization, especially stereolithography, has emerged as a key technology. It employs ultraviolet (UV) light to solidify liquid resins into solid objects, offering a high precision and surface finish [2]. However, while this technique has evolved significantly over the past decade, particularly in the development of composites and nanomaterials, challenges remain, especially concerning the mechanical properties of the printed parts, which are often attributed to the limitations imposed by the viscosity of the resin. Prior research has demonstrated the potential of AM, but the mechanical robustness of photopolymer resins, specifically in medical and dental applications, continues to lag behind expectations, representing a notable gap in the current AM literature [3].

Previous studies have underscored the transformative impact of material innovations, particularly composites and nanomaterials, in overcoming some of these technical barriers. For instance, the introduction of photopolymerization in healthcare in the 1960s and subsequent advancements, such as the incorporation of non-toxic, UV-curable materials in the 1980s, led to significant strides in dental care and implants [4]. Composites enhanced with fillers like silica, ceramics, and natural minerals have demonstrated improved tribological and mechanical properties. However, limited attention has been given to exploring the optimal integration of specific nanomaterials, such as HA, within the context of 3D-printed dental resins. HA, known for its excellent biocompatibility and capacity to bond with human bone, is commonly used in dental and orthopaedic implants, but its full potential in AM applications remains underexplored [5-7].

The mechanical properties of HA are strongly influenced by its synthesis process, with factors such as particle size, crystallinity, and morphology playing crucial roles. While HA nanoparticles enhance mechanical performance and accelerate bone bonding, most research has been focused on bulk applications rather than its use in 3D-printed composites [8]. As a result, there is limited understanding of how small quantities of HA, when integrated into photopolymer resins, affect key mechanical properties such as tensile strength, impact resistance, and frictional behaviour.

The objective of this study is to investigate the effects of incorporating HA nanoparticles into 3D-printed dental photopolymer resins. This research evaluates key mechanical and tribological properties, including tensile strength, impact resistance, Shore D hardness, and wear behavior, while analyzing the morphological structure to understand HA distribution. By exploring the relationship between HA concentration and material performance, this study aims to optimize the mechanical properties of 3D-printed dental resins and provide a foundation for further innovations in AM for healthcare applications. The findings are expected to contribute to the development of high-performance, biocompatible materials, addressing current limitations in resin-based AM and expanding its potential in advanced dental and biomedical applications.

2. MATERIALS AND METHODS

2.1 Material preparation

The eSun dental resin model was selected as the photopolymer resin. Manufactured by eSun Industrial Co., Ltd., an industry leader based in Shenzhen, China, this resin represented a crucial component in the investigation into the impact of the additive on the properties of dental photopolymer resin. The selection of the eSun dental resin model underscores its prevalence and significance in the 3D printing landscape, as well as its potential role in dental applications, given its specialised formulation that is tailored for the creation of dental models

The HA nanoparticles employed as the reinforcing agent in this research were meticulously produced by Xi'an Best Bio-Tech Co., Ltd. These HA nanoparticles, which are characterised by a diameter of 20 nm and an impressive purity level of 99%, offer a highly refined and consistent material for integration into the dental resin matrix. The decision to use HA nanoparticles as an additive came from their proven efficacy in enhancing the mechanical properties of materials, especially when used in controlled concentrations.

The deliberate inclusion of HA nanoparticles as an additive in this study served to explore the nuanced effects of their incorporation into the eSun dental resin model. The research strategically investigated varying concentrations of HA nanoparticles, namely 1, 3, and 5 wt.% (mass fraction), to comprehend their dose-dependent impact on the material properties. This methodical approach allowed for a comprehensive examination of the response of the resin to different levels of nanoparticle incorporation, shedding light on the optimal concentration for achieving the desired enhancement in properties such as frictional resistance, tensile strength, and impact strength.

In essence, the research design was not only aimed at elucidating the potential of HA nanoparticles as a reinforcing agent but also sought to contribute valuable insights into the formulation of a dental photopolymer resin tailored for 3D printing. By precisely controlling the concentration of HA nanoparticles, the study aimed to unlock a nuanced understanding of the intricate interplay between the additive and the resin, paving the way for informed decisions in optimising the material for dental applications within the dynamic realm of AM.

The initial stage in the preparation of the material for use in this research was the process of mixing the two materials (dental resin and HA). The resin and HA nanoparticles were mixed using a magnetic stirrer for around 15 minutes. Subsequently, this mixture was placed into an ultrasonic mixer (NTL-UC411) with ultrasonic parameters of 40 kHz and 60 W for 90 minutes. Homogeneity in the nanoparticle mixture was easily achieved by employing a simple method to mix the photopolymer-type resin, followed by the use of an ultrasonic mixer.

The next step after the material mixing process was the printing process. However, several things had to be considered before the printing process could be carried out. The tool preparation was accomplished using a Halot Box resin slicer. The settings were a layer height of 0.05, motor speed of 5 mm/s, initial exposure time of 40 s, lift distance of 8 mm, and a bottom layer of two. The samples for the tests were prepared according to predetermined standards. The printer of choice was a stereolithographic 3D printer. The printer software was then used to slice the sample design. Each variant was comprised of five samples, with an average of five test datasets.

Before entering the testing stage, material density calculations were done because the material used was not a general material or a fabricated commercial product as it involved the addition of HA to the resin material. Density calculations and checks were conducted to determine the density of the specimens. The theoretical density and mixture density were calculated using Equations (1) and (3). The mixture density was calculated using the volume fraction obtained with the mass fraction conversion in Equation (2). The porosity of the specimens was calculated using Equation (4). The density equation formula was used for the density calculations by weighing the mass and measuring the specimens.

$$\rho_a = \frac{M_a}{V_a} \tag{1}$$

$$V_f = \frac{\rho_m w_f}{\rho_f(1-w_f)+\rho_m w_f} \tag{2}$$

$$\rho_c = \rho_m V_f + \rho_m(1 - V_f) \quad (3)$$

$$\%P = 1 - \frac{\rho_a}{\rho_c} \times 100\% \quad (4)$$

where, ρ_a is the specimen's density (g/cm^3), M_a is the specimen's actual mass, (g), V_a is the specimen's actual volume (cm^3), V_f is the specimen's volume fraction, ρ_m is the matrix's density (g/cm^3), ρ_f is the filler's density, (g/cm^3), w_f is the filler's mass fraction, ρ_c is the composite's density (g/cm^3), $\%P$ is the composite's porosity percentage, and ρ_a is the composite's actual density (g/cm^3).

2.2 Material characterization

Characterisations, such as tensile, impact, SEM, and tribology tests, were conducted to understand the mechanical, morphological and tribological properties of the material. The tensile test was aimed at measuring the strength and resistance of the material to tensile loads. This was useful in determining the elastic modulus, elastic limit, maximum tensile strength, and maximum strain of the material. The response of the material to the applied stress was also determined. The tensile test followed the ASTM D638-14 Type 5 standard, utilising a withdrawal speed of 1 mm/min and a load cell of 200 kg. The average of five samples for every variation was taken as the tensile strength.

Next, impact testing was conducted to determine the toughness and quality of the energy absorption of the material. Impact testing was important in this research as it is related to the ability of a material to absorb energy suddenly. This test is also beneficial for determining the strength of a material to withstand fracture and cracking, evaluating the behaviour of a material under dynamic or shock loads, as well as analysing interactions under dynamic loads. The energy absorption capability was evaluated using the Izod pendulum impact test and performed following the ASTM D4812-99 standard.

Meanwhile, to obtain an overview of the micro and nano levels of the composites, micrograph tests were conducted to determine the morphology, grain size, phase distribution and composition of the materials used. Defects were also identified. All this was done to gain an understanding of the surface structures that can influence the mechanical and tribological properties of materials. The fracture structure obtained from the tensile test results could observed in the photos acquired via SEM. The process involved preparing specimens measuring 5x5 mm^2 and placing them in a vacuum chamber to remove impurities. Figure 1 shows the SEM used.

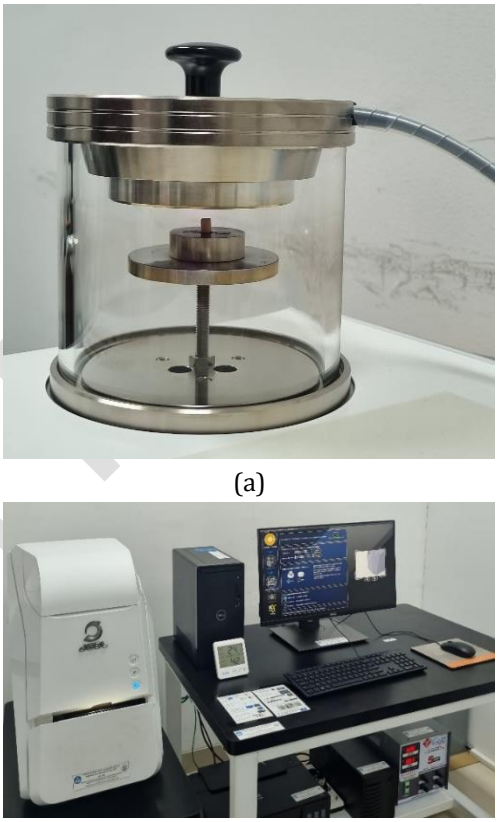

(a)

(b)

Fig. 1. Scanning electron microscope; (a) coating process using platinum; (b) testing process.

Shore D hardness tests were conducted to measure the hardness of the polymer materials. This test can be used to determine the hardness level of a material against indentation and its hardness distribution. In addition, this test is designed to establish the relationships between material hardness and other tests performed, particularly the wear resistance of a material. In this study, the hardness tests were performed using the HD testing method according to ASTM D2240 with five test points.

The final test was the friction test, which is related to the understanding of tribology in terms of analysing the interaction of friction and wear between two relatively moving surfaces. This test

measures the coefficient of friction (μ) and material wear (K) and evaluates lubricity and wear resistance. It is important to understand the properties of the materials used in applications involving friction and wear. The K test was conducted using a pin-on-disc tribometer machine following ASTM G99 using parameters of velocity at 2 m/s, nominal load of 2 kg, and track length of 1800 m. The friction testing and tools used are shown in Figure 2.

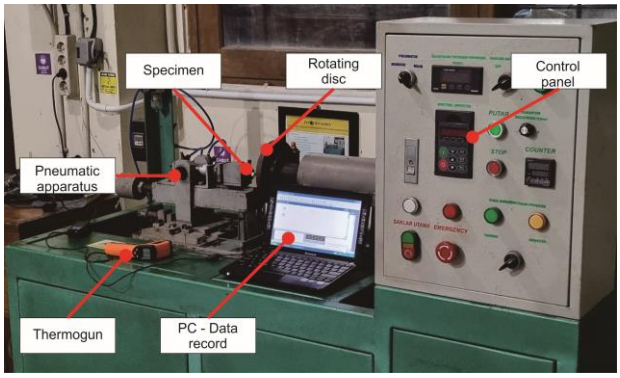

Fig. 2. Tribometry machine.

The test was based on calculations using the equation of K and volume change (ΔV) in the material. The equation used is an equation that is specifically intended for testing using the pin-on-disc method. The K of the material was obtained using Equation (5), while Equation (6) was used to calculate the ΔV. Once both values were obtained, the μ could be determined through Equation (7).

$$K = \frac{\Delta V}{F \,.\, L} \quad (5)$$

$$\Delta V = \frac{m_1 - m_2}{\rho} \quad (6)$$

$$\mu = \frac{f}{N} \quad (7)$$

where, K is the material's wear rate (mm^3/Nm), ΔV is the volume change of the pin specimen (mm^3), F is the pressing force or normal force that occurs on the specimen (N), and L is the length of the path traversed by the pin specimen over a certain period of time (m), m_1 is the material's mass pre-testing (grams), m_2 is the material's mass post-testing (grams), and ρ is the material's density ($grams/mm^3$), μ is the specimen's coefficient of friction, f is the amount of frictional forces that occur when the pin and disc specimens rub together, and N is the normal force exerted on the specimen during testing.

3. RESULTS AND DISCUSSION

3.1 Tensile test

The discernible impact of the HA nanoparticles on the tensile strength of the dental photopolymer resin models, as evidenced by this study, unveiled a critical aspect of material behaviour with significant implications for dental applications [10-12]. The investigation into 0, 1, 3, and 5 wt.% mass fractions of HA nanoparticles shed light on the dose-dependent correlation between the incorporation of nanoparticles and the enhancement of tensile strength.

The observed increases of 12.7%, 12.8%, and a substantial increase of 44.6% in the tensile strength of the 1, 3, and 5 wt.%-resin-HA (RHA) composites, respectively, showcased the pronounced reinforcing effect of the HA nanoparticles on the resin matrix (Figure 3). The resulting tensile strength values of 51.53, 51.605, and 66.11 MPa, respectively, underscored the transformative potential of HA as a strengthening agent for dental resin models. Notably, the maximum tensile strength of 66.11 MPa in the 5 wt.%-RHA signified a remarkable improvement of 44.6% from the baseline strength of 45.72 MPa.

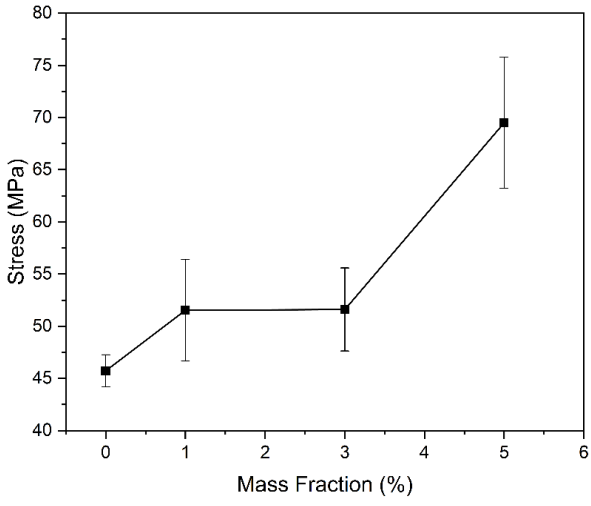

Fig. 3. Tensile Strength of resin-HA Composite.

The mechanism behind this observed increase in tensile strength could be attributed to several factors. Firstly, the addition of HA nanoparticles reduced stretching within the resin, leading to increased mechanical strength. This reduction in stretching could be linked to

the augmented molecular rigidity of the HA nanoparticles, which effectively limited the extent of deformation under tensile loading conditions. Secondly, the increased HA ratio, particularly at higher mass fractions, played a role in fortifying the resin matrix. The higher concentration of HA nanoparticles created a denser network within the resin, reinforcing its structural integrity and enhancing its overall tensile strength. The mechanical interlocking effect between the HA nanoparticles and the resin was crucial in elucidating the observed improvement in tensile strength. This interfacial interaction created a cohesive bond between the HA and resin, resulting in a synergistic strengthening that surpassed the capabilities of the resin without the incorporation of nanoparticles. The mechanical interlocking effect promoted an enhanced load transfer within the material, effectively distributing the stress and preventing premature failure.

The results of this test were also employed to study the stress-strain variations in the materials used against the pure material. Figure 4 shows the stress-strain graph for each variation. The test results showed that although the addition of HA was able to increase the tensile strength, the strain was lower. The maximum tensile strength was obtained by the 5 wt.%-RHA. However, this material was less stretchable than the pure material without any additives. In the two types of variations, the stress-strain almost appeared to be the same. This could have been due to a poor mixing process.

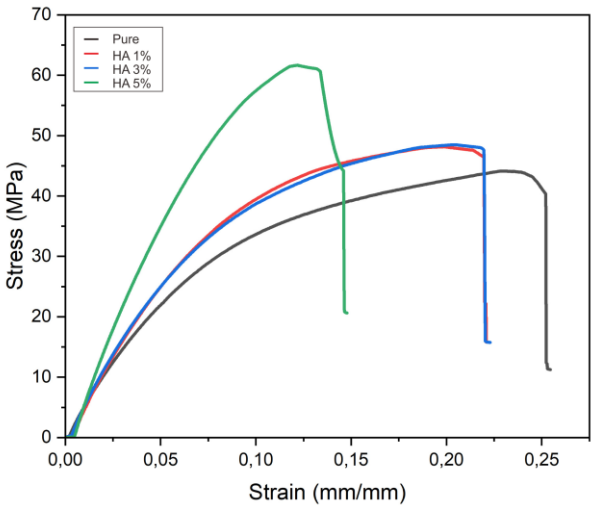

Fig. 4. Stress-strain graph of HA-resin specimen.

In essence, the study highlighted the intricate interplay between the HA nanoparticles and the mechanical properties of the dental photopolymer resin. The substantial improvement in tensile strength underscored the potential of HA as a reinforcing agent, offering a pathway to develop dental materials with enhanced mechanical performance. As the dental industry increasingly adopts 3D printing for various applications, these findings will contribute valuable insights toward optimising material formulations, emphasising the significance of the incorporation of HA nanoparticles to achieve superior tensile strength in dental resin models [13].

The Halpin-Tsai-Pagano Equations (8), (9), and (10) were used to calculate the elastic modulus of the RHA composites. The Halpin-Tsai equation is a mathematical model that can be used to predict the elastic modulus of a composite based on the geometric shape, orientation of the filler, and the elastic properties of the filler and matrix [14].

$$\frac{Em_1}{Em} = \frac{1+\xi\eta VHA}{1-\eta VHA} \tag{8}$$

$$\eta = \frac{\frac{EHA}{Em}-1}{\frac{EHA}{Em}+1}$$

$$\frac{Em_2}{Em} = \frac{1+\xi\eta VHA}{1-\eta VHA} \tag{9}$$

$$\eta = \frac{\frac{EHA}{Em}-1}{\frac{EHA}{Em}+2}$$

$$E_t^c = \frac{3}{8}\,Em_1 + \frac{5}{8}\,Em_2 \tag{10}$$

where, Em_1 is the RHA's transverse elastic modulus, Em_2 is the RHA's longitudinal elastic modulus, E_t^c is the Halpin-Tsai-Pagano elastic modulus, Em is the resin's elastic modulus, and EHA is the HA nanoparticles' elastic modulus, while, ξ and VHA are the geometry and volume fraction of the HA nanoparticles, respectively.

The tensile test results obtained were then used to analyse and validate the theoretical elastic modulus. In this case, the EHA was compared with the Em_1, Em_2, and E_t^c [14]. The results of the comparison of elastic modulus values are shown in Figure 5.

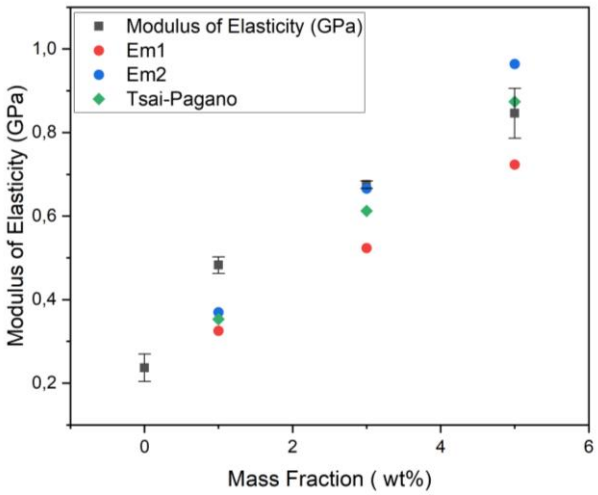

Fig. 5. Experimental and theoretical modulus of elasticity.

Figure 5 shows the differences between the theoretical and experimental elastic modulus. The experimental results of mixing resin with HA nanoparticles did not match the theoretical elastic modulus values. For the 1 wt.%-RHA, the theoretical elastic modulus values, based on the Em_1, Em_2, and E_t^c, were respectively, 48, 30, and 37% lower than the experimental results. On the other hand, for the 3 wt.%-RHA, the experimental elastic modulus was greater than the Em_1 (29%), while it was closer to the theoretical Em_2 and E_t^c with a difference of 1 and 10%, respectively. For the 5 wt.%-RHA, there was a difference between the experimental and theoretical results, where the theoretical Em_1 was 17% lower while the Em_2 was 12% higher than the experimental results. The E_t^c was close to the experimental elastic modulus, which was 3% higher.

The difference between the experimental and theoretical results could have been caused by the inability of the Tsai-Pagano method to predict perfection during the mixing process, the saturation points of the addition of HA nanoparticles, the effect of the uneven distribution of nanoparticles, the bonds between atoms, the defects when the printing process used UV light, and the possibility of the occurrence of structural changes. On the other hand, apart from the significant differences between the theoretical and experimental results, the Halpin-Tsai-Pagano method was able to correctly predict the trend of increasing elastic modulus that occurred when the resin was treated with HA nanoparticles.

3.2 Impact test

Figure 6 shows the results of the material impact testing. In the absence of HA nanoparticles (0 wt.%), the resin specimen demonstrated an impact strength of 20.75 kJ/m^2, serving as a pivotal reference point for subsequent comparisons with samples incorporating HA nanoparticles. The introduction of HA nanoparticles at mass fractions of 1, 3, and 5 wt.% led to remarkable enhancements in the impact strength, showcasing the potential of these nanoparticles as reinforcing agents within the resin matrix.

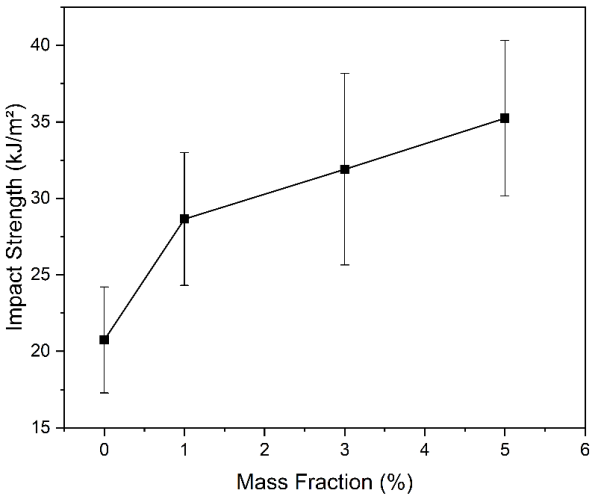

Fig. 6. Impact strength of resin-HA composite.

Specifically, the impact strength exhibited substantial increases of 38.1, 53.7, and 69.8%, resulting in impact strengths of 28.6, 31.9, and 35.2 kJ/m^2, respectively. These findings highlighted a dose-dependent correlation between the concentration of HA nanoparticles and the resultant improvement in impact strength. Notably, the 5 wt.%-RHA stood out as the composite with the most significant increase in impact strength, underscoring the effectiveness of higher concentrations of nanoparticles in augmenting the resistance of a material to impact forces.

The observed trend in impact strength could be attributed to the reinforcing effect of the HA nanoparticles on the resin matrix. The incorporation of HA nanoparticles, particularly at higher concentrations, enhanced the ability of the material to absorb and distribute the impact energy [15,16]. This could be attributed to several factors, including the increased molecular

rigidity, improved interfacial interactions between the HA nanoparticles and resin, and the formation of a denser network within the material. These factors collectively contributed to the observed improvement in impact strength, emphasising the pivotal role of the HA nanoparticles in fortifying the resin against sudden and dynamic loading conditions [17].

These findings not only provide valuable insights into the impact resistance of the dental photopolymer resin but also open avenues for the further optimisation of material formulations. As the concentration of the HA nanoparticles emerged as a critical factor in determining the impact strength, future research may delve deeper into refining the balance between the nanoparticle concentration and material performance. The demonstrated ability of the HA nanoparticles to significantly enhance the impact strength holds promise for advancing the resilience of dental resin models, an essential consideration in applications where resistance to sudden forces is paramount, such as for dental prosthetics and implant components.

This increase in impact strength is associated with the transfer of stress at the interface and the compatibility between the nanoparticles and resin [18]. The inclusion of nanoparticles can enhance the impact resistance and mechanical properties of a material owing to the reinforcing effect, which toughens the material. Additionally, the interactions between the resin and nanoparticles, specifically the interfacial adhesive strength and stiffness, play a crucial role in the transfer of stress and can enhance the mechanical performance of the material, including its impact strength [19].

3.3 Hardness test

A hardness test was conducted to assess the surface hardness of the resin with and without the addition of HA nanoparticles. In addition, the hardness properties of the resin could have influenced the outcomes of the other mechanical tests, and therefore, a hardness test was conducted to support the data and discussions. The results of the hardness test indicated that the material was resistant to plastic deformation, which was inherently linked to the strength and durability of the material. Furthermore, the data obtained from the hardness test could be utilised to evaluate the effectiveness of the HA nanoparticles as reinforcing and enhancing agents to determine the optimal values for composite fabrication.

Figure 7 illustrates the HD test results for each resin variation. These results indicated that there was an overall increase in hardness in the resins with the addition of the HA nanoparticles. The HD of the 0 wt.%-RHA was 72.96. In contrast, the HD of the 5 wt.%-RHA was 79.32, indicating an increase of 8.7%. Conversely, for the 1 wt.%- and 3 wt.%-RHA, there was an insignificant increase of 0.27 from 74.54 to 74.74.

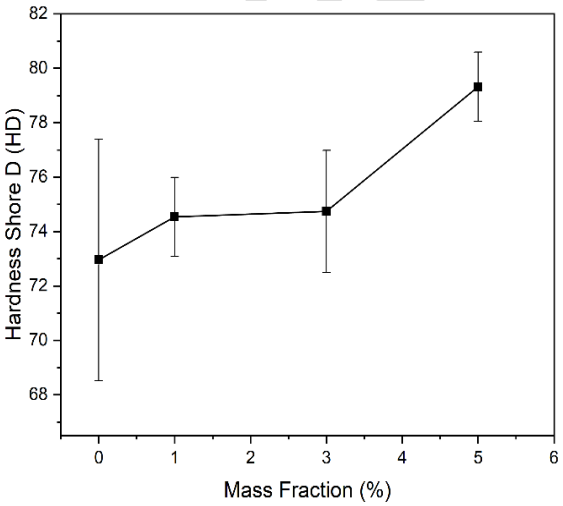

Fig. 7. Hardness Shore D of resin-HA composite.

Hydroxyapatite (HA) is a bioceramic with similar properties to bone and is characterised by its hardness. So, the addition of HA at concentrations of 1, 3, and 5 wt.% would increase the hardness of a resin. Conversely, HA has anti-deformation properties that could increase the brittleness of the resin with the addition of HA. The hardness of the RHA was directly proportional to the increase in wear resistance of the composite. Therefore, it was concluded that the hardness of the RHA affected the results of the water absorption rate tests. The significant increase in hardness due to the addition of nanoparticles could be attributed to the (a) uniform distribution of nanoparticles in the matrix, (b) increased density of dislocations in the composite, (c) increased number of hard nanoparticles in the matrix, which contributed to the increased hardness of the composite, according to the law of mixing [20].

Smaller-sized particles, such as nanoparticles, will result in increased interfacial shear stress, which is required for dislocation to occur. The Hall-Petch theory states that the smaller the particle or grain size, the greater the yield strength of the material. This is similar to the strengthening of grain boundaries to influence the interfacial phase, resulting in increased mechanical strength such as hardness. Thus, the increased hardness of the composite was related to the particle size of the composite reinforcement [21].

3.4 Surface morphology

An analysis using scanning electron microscopy (SEM) was used to investigate the morphological structure of the fracture surface during tensile testing with and without the addition of HA nanoparticles. The resulting SEM micrographs (Figure 8) provided a more robust interpretation of the results of the tensile tests. The SEM testing was conducted on the 0 wt.%-RHA specimen as a reference, Specimen #2 from the 1 wt.%-RHA variation as the specimen with the lowest tensile strength, and Specimen #2 from the 5 wt.%-RHA variation as the specimen with the highest tensile strength.

On the micrograph of the surface of the structure, roughness was marked by the presence of microcracks (a) and longitudinal fractures or large microcracks (c). These fault gaps indicated the phenomena of microcracks and large microcracks. The rough surface was due to the addition of nanoparticles to the resin, and the presence of internal fracture gaps indicated an increase in the strength of the material [22].

The micrograph of the structure indicates that the surface of the 0 wt.%-RHA specimen was tidy, and the fracture gap was flat and smooth (Figure 8a). In Figures 8b and 8c, it is evident that the addition of HA nanoparticles made the fracture surface rougher, and clumps, which could be in the form of HA nanoparticles or platinum coagulation obtained during the SEM photo-coating process, were visible. In the 1 wt.%-RHA, it can be seen that the surface was not much different from that of the 0 wt.%-RHA specimen due to the addition of low levels of HA nanoparticles (Figure 8b). Conversely, Figure 8c demonstrates that the 5 wt.%-RHA displayed a coarser surface with a significant crack and more profound fracture gap compared to both the 0 wt.%- and 1 wt.%-RHA [22,23]. The SEM photographs depict a surface with both shallow and deep fracture gaps, indicative of roughness. These gaps corresponded to the phenomena of micro and large cracks. The addition of nanoparticles to the resin caused the surface to become rougher, leading to an increase in material strength, as demonstrated by the presence of deep fracture gaps [23].

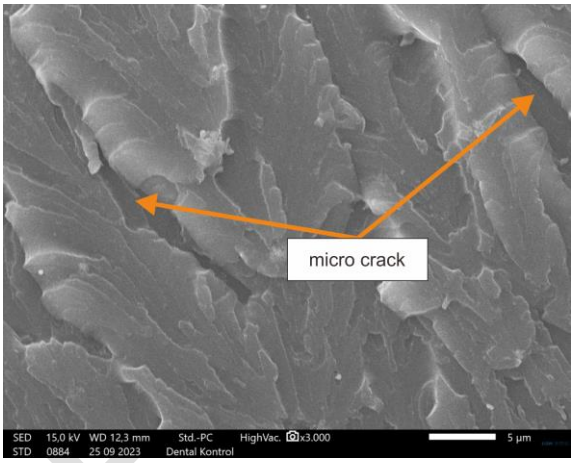

(a)

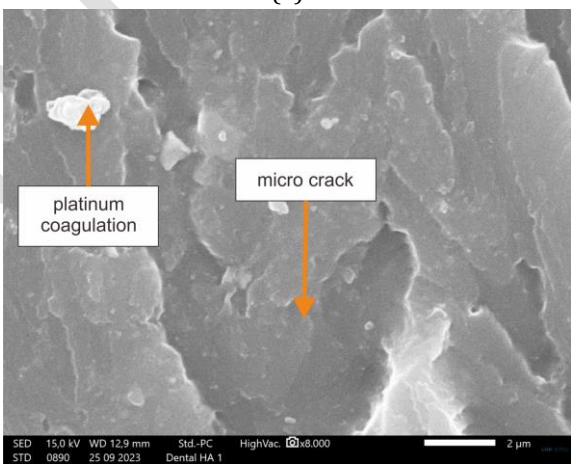

(b)

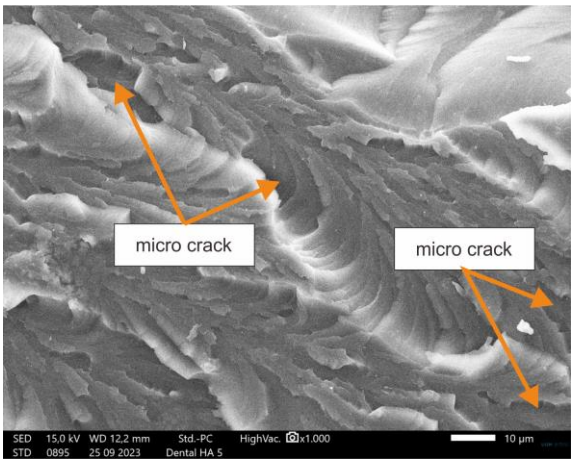

(c)

Fig. 8. SEM Photograph; (a) Figure 6. SEM Photograph of Pure Dental Model Photopolymer Resin; (b) Resin-HA 1 wt%; and (c) Resin-HA 5 wt%

3.5 Wear rate test

The observed decrease in the *K* of the 0, 1, 3, and 5 wt.%-RHA specimens is a significant finding that underscores the potential for improving the durability of dental photopolymer resin models (Figure 9). The specific *K* values recorded at each concentration provided a quantitative measure of the response of the material to frictional loading, revealing a consistent trend of reduced wear as the mass fraction of HA nanoparticles increased.

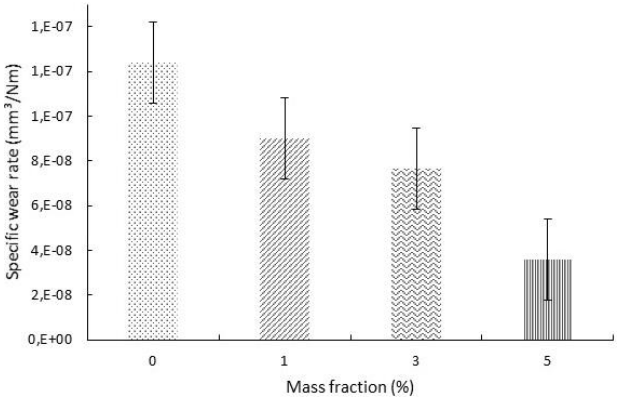

Fig. 9. Specific wear rate of resin-HA composite.

The specific *K* values of 1.24×10^{-7}, 9.02×10^{-8}, 7.65×10^{-8}, and 3.60×10^{-8} mm^3/Nm for the 0, 1, 3, and 5 wt.%-RHA specimens, respectively, demonstrated a notable enhancement in wear resistance with higher concentrations of HA. This trend was particularly pronounced in the 5 wt.%-RHA, where the *K* was the lowest. The substantial reduction in *K* was indicative of the synergistic effect between the HA nanoparticles and the resin matrix, suggesting that the incorporation of HA imparted a protective mechanism against wear and abrasion.

The correlation between material hardness and wear resistance is a well-established principle in materials science, and the results were aligned with this understanding. The addition of HA nanoparticles led to an increase in the hardness of the resin, thereby influencing the specific *K*. This phenomenon was further elucidated by the high anti-deformation properties inherent in HA nanoparticles, allowing them to absorb a significant portion of the load during frictional loading [24-26]. Moreover, the impact on shear stress during the wear process was a critical aspect of the observed reduction in *K*. The increased hardness resulting from the incorporation of HA enhanced the scour resistance of the resin surface, mitigating the shear stress between the resin/HA and the rotating disc. This reduction in shear stress was pivotal in slowing down the wear speed as the primary material, the resin, was subjected to minor stresses. The interplay between the hardness, anti-deformation properties, and shear stress reduction collectively contributed to the enhanced wear resistance of the dental photopolymer resin model [27,28]. These findings not only validate the potential of the HA nanoparticles as an effective additive for improving wear resistance in dental photopolymer resins but also offer valuable insights into the underlying mechanisms governing the observed behaviour. This knowledge holds promise for the advancement of dental materials tailored for 3D printing applications, emphasising the importance of optimising material formulations for enhanced performance in the demanding conditions of dental applications.

The results of the tests conducted with the pin-on-disc were then analysed by the stability of the μ over the test duration. A total of 800 data was collected. Figure 10 shows that the friction test results were stable. The test results showed that all the data variations showed values of μ that tended to be stable throughout the test and that the 1 wt.%-RHA appeared to be more stable compared to the other specimens. However, the point distribution showed the same pattern. As could be seen in one case in data 171 to 209, there were prominent values for all the RHA specimens. Meanwhile, the pure pattern did not show any such differences. This was thought to be the result of the less uniform mixture results in the part of the sample where HA was added. Apart from that, the data from 418 to 513 in all the samples showed the same pattern. Thus, the process and method of adding HA to each variation had a good level of stability.

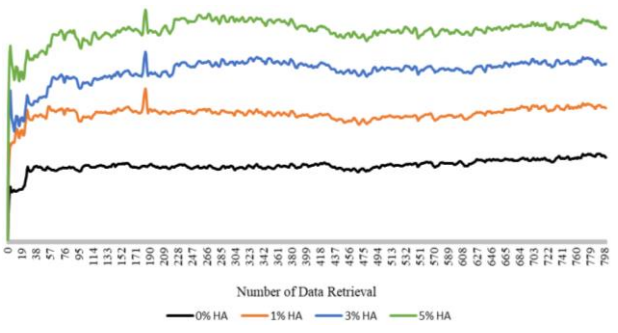

Fig. 10. The stability of all sample friction coefficient

Figure 11 shows the effect of the mass fraction on the μ. Overall, the μ of all the samples decreased. The μ of the 0 wt.%-RHA was 0.844. On the other hand, the μ of the 1, 3, and 5 wt.%-RHA decreased by 39.9, 44.1, and 47.8%, respectively, with μ values of 0.506, 0.471, and 0.439. The 5 wt.%-RHA had the smallest μ. The addition of HA nanoparticles was able to increase the surface hardness of the resin. Surface hardness had a significant influence on the tribological properties (K and μ) of the resin. The higher the surface hardness of the resin, the lower the μ [29]. Smaller particle sizes can increase wear resistance and reduce friction. In addition, smaller particle sizes can effectively prevent the formation of surface defects and wrinkles that cause increased surface friction [30].

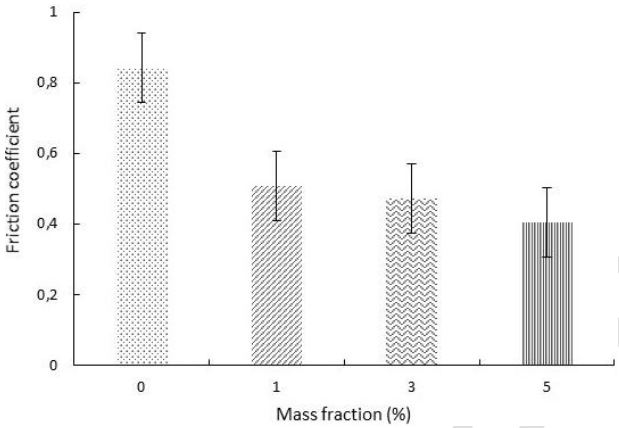

Fig. 11. Relationship between mass fraction and friction coefficient.

The relationship between the mass fraction of HA nanoparticles and the friction coefficient (μ) is pivotal in understanding the interconnection between the mechanical and tribological performance of the resin composites. In this study, the inclusion of HA nanoparticles significantly reduced the coefficient of friction, with the 5 wt.% HA sample demonstrating the lowest values. This improvement in tribological behavior is directly linked to the enhancements in mechanical properties, such as tensile strength, impact resistance, and Shore D hardness. For instance, the increased hardness and tensile strength minimize material deformation and detachment during sliding contact, thereby reducing both the wear rate (K) and μ.

The dual role of HA nanoparticles within the resin matrix further explains this relationship. At lower concentrations, HA particles are well-dispersed, leading to improved load-bearing capacity and reduced material deformation during tribological interactions. This dispersion also promotes effective mechanical interlocking, enhancing the composite's ability to withstand localized compressive stresses. However, as the mass fraction increases, the risk of particle agglomeration rises, which may disrupt uniform frictional behavior by creating localized stress concentrations. Nevertheless, even at higher concentrations, HA's ability to act as micro-lubricants during sliding contact reduces direct asperity interactions, contributing to smoother wear tracks and smaller debris particles.

Morphological analysis of the tribocontact zones (SEM) provides further insights into these mechanisms. For HA-free samples, extensive plowing marks and large debris particles were observed, indicating severe abrasive wear and insufficient material hardness. In contrast, the HA-reinforced samples exhibited finer debris and smoother wear tracks, which highlight the reinforcing effect of HA in enhancing both surface hardness and wear resistance. The debris analysis underscores this interplay, showing that higher HA content correlates with smaller, more uniformly distributed debris. This finding suggests that HA nanoparticles improve the composite's ability to resist fracture and mitigate material transfer during sliding, directly influencing the wear and friction properties.

Despite these advantages, excessive HA content may lead to diminishing returns in friction reduction due to increased brittleness. While higher HA concentrations enhance wear resistance and hardness, they can also reduce the material's flexibility, potentially impacting its overall mechanical robustness. This balance between hardness and flexibility must be carefully optimized to achieve the desired tribological performance without compromising other mechanical properties.

The integration of SEM micrographs of the tribocontact zones into the analysis provides visual evidence supporting these findings. The images illustrate a clear transition from adhesive to abrasive wear as HA concentration increases, further confirming the hypothesis that HA's reinforcement capabilities significantly influence both mechanical and tribological behavior.

Future studies could explore variations in HA particle size, surface characteristics, or morphology to better understand their dynamic influence on debris formation and contact mechanics in real-time tribological testing.

4. CONCLUSION

The K test results indicated that the K and μ of all the samples decreased. The 5 wt.%-RHA had the lowest K (3.60×10^{-8} mm^3/Nm) and μ (0.439), while the 0 wt.%-RHA had the highest K ($1.24 \times 10^{-7} mm^3/Nm$) and μ (0.506). The mechanical testing, which included tensile and impact testing, found that the mechanical properties of the material increased with the addition of HA nanoparticles. The highest tensile strength (66.11 MPa) was observed in the 5 wt.%-RHA, while the lowest (45.72MPa) was found in the 0 wt.%-RHA. Similarly, the impact strength also increased after the addition of HA nanoparticles. The highest impact strength (35.2 kJ/m^2) was in the 0 wt.%-RHA and the lowest (20.75 kJ/m^2) was in the 5 wt.%-RHA. The same trend was observed in the HD test results, with the highest and lowest HD being observed in the 5 wt.%-RHA (79.32) and 0 wt.%-RHA (72.96), respectively. Lastly, the SEM results indicated that the addition of HA nanoparticles affected the surface of the specimens by causing larger microcracks, thus suggesting an enhancement in mechanical properties.

Author Contributions

Conceptualization, K.D., U.U., and J.T.; methodology, R.R. and F.I..; software, A.H.; validation, U.U., E.S. and S.B.C.; formal analysis, R.R.; investigation, R.R., B.W.L., and A.H.; data curation, U.U. and S.B.C`.; writing—original draft preparation, R.R.; writing—review and editing, R.R. and B.W.L.; visualization, R.R. and A.H.; supervision, K.D., U.U., J.T., E.S., and S.B.C.; All authors have read and agreed to the published version of the manuscript.

Acknowledgement

Authors thank to Universitas Sebelas Maret for the financial funding under research grant PT 2024.

REFERENCES

[1] S. Park, W. Shou, L. Makatura, W. Matusik, and K. Fu, "3D printing of polymer composites: Materials, processes, and applications," *Matter*, vol. 5, no. 1, pp. 43–76, Jan. 2022, doi: 10.1016/j.matt.2021.10.018

[2] A. Bagheri and J. Jin, "Photopolymerization in 3D printing," *ACS Applied Polymer Materials*, vol. 1, no. 4, pp. 593–611, Feb. 2019, doi: 10.1021/acsapm.8b00165

[3] E. Matias and B. Rao, "3D printing: On its historical evolution and the implications for business," 2022 Portland International Conference on Management of Engineering and Technology (PICMET), Aug. 2015, doi: 10.1109/PICMET.2015.7273052

[4] R. Yadav, H. Lee, J.-H. Lee, R. K. Singh, and H.-H. Lee, "A comprehensive review: Physical, mechanical, and tribological characterization of dental resin composite materials," *Tribology International*, vol. 179, p. 108102, Nov. 2022, doi: 10.1016/j.triboint.2022.108102

[5] X. Liang MA, "Research on application of SLA technology in the 3D printing technology," *Applied Mechanics and Materials*, vol. 401–403, pp. 938–941, Sep. 2013, doi: 10.4028/www.scientific.net/AMM.401-403.938

[6] J.W. Stansbury, "Curing dental resins and composites by photopolymerization," *J. Esthet. Dent.*, vol. 12, no. 6, pp. 300-8, 2000. doi: 10.1111/j.1708-8240.2000.tb00239.x

[7] Z. J. H. Al-Bahar, "Evaluation The Effect of Incorporated Hydroxyapatite Prepared From Dried Egg Shell On Some Properties Of Relined Denture Base," 2012. [Online]. Available: https://www.uomosul.edu.iq/public/files/datafolder_30/oldUo_20190816_052507_88_54.pdf

[8] Dasgupta, S. Tarafder, A. Bandyopadhyay, and S. Bose, "Effect of grain size on mechanical, surface and biological properties of microwave sintered hydroxyapatite," *Materials Science and Engineering C*, vol. 33, no. 5, pp. 2846–2854, Mar. 2013, doi: 10.1016/j.msec.2013.03.004

[9] M. F. Fardan, B. W. Lenggana, U. Ubaidillah, S.-B. Choi, D. D. Susilo, and S. Z. Khan, "Revolutionizing Prosthetic Design with Auxetic Metamaterials and Structures: A Review of Mechanical Properties and Limitations", *Micromachines*, vol. 14, no. 6, p. 1165, May 2023, doi: 10.3390/mi14061165.

[10] S. Aydin, B. Kucukyuruk, B. Abuzayed, S. Aydin, and G. Z. Sanus, "Cranioplasty: Review of materials and techniques," *Journal of Neurosciences in Rural Practice*, vol. 02, no. 02, pp. 162–167, Jul. 2011, doi: 10.4103/0976-3147.83584

[11] S. A. X. Stango and U. Vijayalakshmi, "Synthesis and characterization of hydroxyapatite/carboxylic acid functionalized MWCNTS composites and its triple layer coatings for biomedical applications," *Ceramics International*, vol. 45, no. 1, pp. 69–81, Sep. 2018, doi: 10.1016/j.ceramint.2018.09.135

[12] D. Sidane et al., "Study of the mechanical behavior and corrosion resistance of hydroxyapatite sol–gel thin coatings on 316 L stainless steel pre-coated with titania film," *Thin Solid Films*, vol. 593, pp. 71–80, Sep. 2015, doi: 10.1016/j.tsf.2015.09.037

[13] Q. Wang, J. Liu, and S. Ge, "Study on biotribological behavior of the combined joint of COCRMO and UHMWPE/BHA composite in a hip joint simulator," *Journal of Bionic Engineering*, vol. 6, no. 4, pp. 378–386, Dec. 2009, doi: 10.1016/S1672-6529(08)60139-0

[14] F. X. Espinach, F. Julián, M. Alcalà, J. Tresserras, and P. Mutjé, "High stiffness performance Alpha-Grass Pulp fiber reinforced thermoplastic Starch-Based fully biodegradable composites," *BioResources*, vol. 9, no. 1, Dec. 2013, http://hdl.handle.net/10256/12325

[15] M. R. Kaimonov, T. V. Safronova, Y. Y. Filippov, T. B. Shatalova, and I. I. Preobrazhenskii, "Calcium Phosphate Powder for Obtaining of Composite Bioceramics", *Inorganic Mater.: Appl. Res.*, vol. 12, no. 1, pp. 34–39, Jan. 2021, doi: 10.1134/s2075113321010135

[16] D. O. Obada, E. T. Dauda, J. K. Abifarin, D. Dodoo-Arhin, and N. D. Bansod, "Mechanical properties of natural hydroxyapatite using low cold compaction pressure: Effect of sintering temperature," *Materials Chemistry and Physics*, vol. 239, p. 122099, Sep. 2019, doi: 10.1016/j.matchemphys.2019.122099

[17] S. Prasadh and R. C. W. Wong, "Unraveling the mechanical strength of biomaterials used as a bone scaffold in oral and maxillofacial defects," *Oral Science International*, vol. 15, no. 2, pp. 48–55, Apr. 2018, doi: 10.1016/S1348-8643(18)30005-3

[18] A. Lutanto, U. Ubaidillah, F. Imaduddin, S.-B. Choi, and B. W. Lenggana, "Development of Tiny Vane-type Magnetorheological Brake Considering Quality Function Deployment", *Micromachines*, vol. 14, no. 1, p. 26, Dec. 2022, doi: 10.3390/mi14010026

[19] R. Barbaz-Isfahani, H. Dadras, S. Saber-Samandari, A. Taherzadeh-Fard, and G. Liaghat, "A comprehensive investigation of the low-velocity impact response of enhanced GFRP composites with single and hybrid loading of various types of nanoparticles," *Heliyon*, vol. 9, no. 5, p. e15930, Apr. 2023, doi: 10.1016/j.heliyon.2023.e15930

[20] M. S. G. Gol, A. Malti, and F. Akhlaghi, "Effect of WC nanoparticles content on the microstructure, hardness and tribological properties of Al-WC nanocomposites produced by flake powder metallurgy," *Materials Chemistry and Physics*, vol. 296, p. 127252, Dec. 2022, doi: 10.1016/j.matchemphys.2022.127252

[21] L. Yang, S. Ma, and G. Mu, "Improvements of microstructure and hardness of lead-free solders doped with Mo nanoparticles," *Materials Letters*, vol. 304, p. 130654, Aug. 2021, doi: 10.1016/j.matlet.2021.130654

[22] C. Xiao, Y. Tan, X. Yang, T. Xu, L. Wang, and Z. Qi, "Mechanical properties and strengthening mechanism of epoxy resin reinforced with nano-SiO2 particles and multi-walled carbon nanotubes," *Chemical Physics Letters*, vol. 695, pp. 34–43, Feb. 2018, doi: 10.1016/j.cplett.2018.01.060

[23] A. Albooyeh, P. Soleymani, and H. Taghipoor, "Evaluation of the mechanical properties of hydroxyapatite-silica aerogel/epoxy nanocomposites: Optimizing by response surface approach," *Journal of the Mechanical Behavior of Biomedical Materials/Journal of Mechanical Behavior of Biomedical Materials*, vol. 136, p. 105513, Oct. 2022, doi: 10.1016/j.jmbbm.2022.105513

[24] H. Y. Nezhad and V. K. Thakur, "Effect of Morphological Changes due to Increasing Carbon Nanoparticles Content on the Quasi-Static Mechanical Response of Epoxy Resin," *Polymers*, vol. 10, no. 10, p. 1106, Oct. 2018, doi: 10.3390/polym10101106

[25] H. Fouad, R. Elleithy, and O. Y. Alothman, "Thermo-mechanical, wear and fracture behavior of high-density Polyethylene/Hydroxyapatite nano composite for biomedical applications: Effect of accelerated ageing," *Journal of Material Science and Technology*, vol. 29, no. 6, pp. 573–581, Mar. 2013, doi: 10.1016/j.jmst.2013.03.020

[26] Z. Li, X. Qi, C. Liu, B. Fan, and X. Yang, "Particle size effect of PTFE on friction and wear properties of glass fiber reinforced epoxy resin composites," *Wear*, vol. 532–533, p. 205104, Aug. 2023, doi: 10.1016/j.wear.2023.205104

[27] H. S. Hanandita, U. Ubaidillah, A. R. Prabowo, B. W. Lenggana, A. Turnip, and E. Joelianto, "Static Structural Analysis of Checking Fixture Frame of Car Interior Using Finite Element Method", *Automot. Experiences*, vol. 6, no. 3, pp. 652–668, Dec. 2023, doi: 10.31603/ae.9860

[28] D. J. Callaghan, A. Vaziri, and H. Nayeb-Hashemi, "Effect of fiber volume fraction and length on the wear characteristics of glass fiber-reinforced dental composites," *Dental Materials*, vol. 22, no. 1, pp. 84–93, Jul. 2005, doi: 10.1016/j.dental.2005.02.011

[29] U. Ubaidillah et al., "A new magnetorheological fluids damper for unmanned aerial vehicles," *Journal of Advanced Research in Fluid Mechanics and Thermal Sciences*, vol. 73, no. 1, pp. 35–45, Jul. 2020, doi: 10.37934/arfmts.73.1.3545

[30] Y. Chen, X. Wang, L. Xu, Z. Liu, and K. D. Woo, "Tribological behavior study on Ti–Nb–Sn/hydroxyapatite composites in simulated body fluid solution," *Journal of the Mechanical Behavior of Biomedical Materials/Journal of Mechanical Behavior of Biomedical Materials*, vol. 10, pp. 97–107, Mar. 2012, doi: 10.1016/j.jmbbm.2012.02.017

[31] S. Kong, J. Wang, W. Hu, and J. Li, "Effects of thickness and particle size on tribological properties of graphene as lubricant additive," *Tribology Letters*, vol. 68, no. 4, Oct. 2020, doi: 10.1007/s11249-020-01351-4